CIMAC CONGRESS 25
ZURICH, MAY 19 – 23, 2025

2025 | 132

The effect of the engine's thermal environment on the injection performance of future fuel injectors

Simulation Technologies, Digital Twins and Complex System Simulation

Gangao Lu, Harbin Engineering University

Liyun Fan, Harbin Engineering University
Li Yang, Shang Hai Jiao Tong University&China Shipbuilding Power Engineering Institute Co., Ltd
Hanwen Zhang, Harbin Engineering University
Guowei Bai, Harbin Engineering University
Dongfang Pu, China Shipbuilding Power Engineering Institute Co., Ltd
Youhong Xiao, Harbin Engineering University
Yunpeng Wei, Harbin Engineering University
Bo Li, Harbin Engineering University

ABSTRACT

The global shipping industry's decarbonization targets have brought significant attention to the development of marine ammonia-fueled engines. However, ammonia fuel's unique physical and chemical properties also pose new challenges for the structural design and performance optimization of fuel injection systems. Future fuel injector designs must fully account for the impact of temperature variations. This study establishes a one-dimensional numerical simulation model based on the future fuel injector for ammonia/dimethyl ether engines independently developed by CPGC (CSSC Power Group Co., Ltd). The model incorporates variations in fuel properties and the convective heat transfer process within the injection channel. Additionally, a CFD analysis is employed to refine the convective heat transfer calculations for key chambers further. Using this model, the dynamic behavior and pressure fluctuation characteristics of ammonia fuel injection are analyzed in detail.

The research results indicate that convective heat transfer significantly impacts the injection characteristics of ammonia fuel. Compared with the adiabatic model, the injection temperature of ammonia fuel increased by 11°C, the injection mass flow rate decreased by 17.4%, and the injection timing also changed. Furthermore, an increase in the supply temperature of ammonia fuel reduces the injection mass flow rate and increases the injection response delay. A comparison of the injection characteristics of diesel and ammonia fuel under the same system structure revealed that the difference in injection rates with diesel fuel significantly amplifies the pressure fluctuation amplitude during the injection process. However, this issue can be mitigated by installing a throttling orifice at the control valve outlet to restrict the servo oil supply. The findings of this study provide theoretical support for the structural design and performance optimization of future fuel injectors.

1 INTRODUCTION

Amid the growing concerns over global climate change and environmental pollution, the international community's urgency in reducing greenhouse gas and pollutant emissions has significantly increased. In response, the International Maritime Organization (IMO) and various national governments have implemented stringent environmental policies and regulations to mitigate the emissions of greenhouse gases and pollutants from maritime activities. As a result, the shipping industry faces unprecedented challenges [1]. Fuels such as ammonia and methanol have zero-carbon and low-carbon emission characteristics and have relatively high energy density, which gives them great potential for addressing global warming and reducing greenhouse gas emissions [2]. Ammonia fuel can be stored and transported using existing infrastructure, and it has relatively low liquefaction temperatures and pressures and high energy density, making it economical for marine applications. Therefore, research on the application of ammonia fuel in marine engines has become a priority [3,4].

Ammonia fuel is characterized by its low viscosity, low density, low modulus of elasticity, and high saturation pressure. These distinctive properties introduce new challenges for its application in traditional fuel injection systems [5,6]. During the operation of the main engine, the injector, particularly the nozzle, is subjected to extreme conditions and high temperatures. In the case of diesel engines, the average temperature of the nozzle can reach approximately 255°C, and during transient injection processes, the peak temperature may rise even further [7-9]. Ammonia fuel, with its high saturation pressure in high-temperature environments, is prone to vaporization. Its physical and chemical properties, particularly the density and modulus of elasticity, are susceptible to temperature changes [10]. Under conditions of high-temperature gas in the cylinder and high injection pressure, the ammonia fuel inside the injector typically exists in a high-temperature, high-pressure subcritical state. It transitions to a supercritical state during the injection process. Pressure fluctuations within the injection system may cause phase changes in the ammonia fuel, thereby affecting the stability of the dynamic injection performance of the injection system [11]. Therefore, by considering the impact of temperature on the injection characteristics of the injector, more effective optimization design schemes can be developed during the design phase.

Studies have demonstrated that both the fuel temperature and the ambient temperature in conventional fuel systems significantly influence the injection characteristics of the injector during the injection process, particularly under cold-start conditions. Payri R. et al. [12] analyzed the effects of fuel temperature on the injection rate and duration of a common rail electromagnetic fuel injector by establishing a one-dimensional adiabatic flow simulation model. Their study explained the significant influence of temperature on the injection characteristics of diesel engines under cold-start conditions. Cavicchi, A. et al. [13] compared cold and reference temperature conditions by adjusting the fuel temperature at the high-pressure pump inlet and the injector body temperature. Their findings indicated that thermal effects substantially impact the closing response of the injector’s needle valve. In contrast, the effects on its opening response and steady injection flow rate are relatively minor. Bae, G.H. et al. [14] utilized X-ray imaging to analyze needle valve motion and investigated the impact of fuel temperature, including low-temperature ranges, on injection performance. Their results showed that lower fuel temperatures reduce the needle valve opening speed and accelerate its closing speed by affecting fuel viscosity and bulk modulus, leading to a decrease in fuel injection rate and significant variations in cyclic injection volume. Salvador F.J. et al.[15] analyzed temperature variations during fuel injection under engine-like conditions. Their results demonstrated heat transfer between the fuel and the wall during new injection processes. Once stable injection conditions are reached, the proposed adiabatic flow assumption effectively predicts temperature changes.

The above studies on fuel injection systems mainly focus on common rail fuel systems for automotive engines, and the results show that the cold environment has a more significant effect on the injection performance, and the fuel injection process follows the adiabatic flow assumption under most operating conditions. Low rotational speeds, large injection volume requirements, and extended injection pulse widths typically characterize marine engines [16]. In these systems, the interaction between fuel flow inside the injector and the wall surface lasts significantly longer than in automotive engines [17]. Furthermore, the injector's elongated and narrow flow channels result in a larger effective convective heat transfer area, facilitating heat transfer from the injector’s high-temperature walls to the fuel during the injection process. This heat transfer may cause deviations in the dynamic injection process, rendering it inconsistent with the adiabatic flow assumption. The future fuel injector of the marine low-speed engine is of a pressurized design, where the fuel pressurization and injection process takes place inside the injector, which further increases

the time the fuel spends with the high-temperature wall. The physical and chemical properties of zero-carbon and low-carbon fuels, such as ammonia, dimethyl ether, and methanol, are susceptible to temperature. Therefore, heat transfer phenomena must be considered during the design process, enabling the correction of temperature-induced effects on injection performance and optimizing thermal management strategies in engine design.

Therefore, this paper takes the ammonia/DME future fuel injector designed independently by CPGC(CSSC Power Group Co., Ltd) as the research object and first constructs a prediction model of ammonia fuel properties and, based on this, establishes a one-dimensional simulation model of the ammonia fuel injection system. For the key heat transfer chamber, the local convective heat transfer is calculated by three-dimensional-CFD, and the heat transfer process of the key chamber calculated by one-dimensional calculation is corrected by defining the volume-averaged surface convective heat transfer coefficient. Based on this model, the influence of high-temperature heat transfer on the injector wall on the injection characteristics of ammonia fuel was studied. The difference in injection characteristics of ammonia fuel under the adiabatic flow model and convective heat transfer model was compared, and the influence of different ammonia supply temperatures on injection characteristics was analyzed. Finally, ammonia fuel and diesel fuel are used for calculation under the same injection conditions, and the injection characteristics are compared. This study provides a reference for the thermal design and injection performance optimization of ammonia fuel injection systems.

2 AMMONIA FUEL INJECTION SYSTEM

Figure 1 shows the external structure of the future fuel injector studied in this paper, which adopts the pressurized integrated design to build pressure for the ammonia fuel through the medium-pressure servo oil as the driving source. The pressure amplifier of the fuel is integrated with the needle valve, which controls the fuel injection. The on-off of the servo oil is realized by the external large flow two-position three-way control valve group to control ammonia fuel's pressure building and injection process effectively. In addition, to meet the unique needs of future fuels such as ammonia, a special sealing and forced lubrication structure is designed in the injector. Future fuel's low-pressure supply circuit and low-pressure servo oil system will be used to solve the problem of fuel leakage in the high-pressure chamber during pressure building and injection and effectively reduce the wear of moving parts caused by low-viscosity fuel. Finally, taking into account the fuel injection requirements under different operating conditions of the main engine, devices such as purge control valves and fuel switching valves for future fuel are designed to ensure the safety of the future fuel circuit in the injection system after switching fuel modes of the main engine, and at the same time to meet the cooling requirements of the injector.

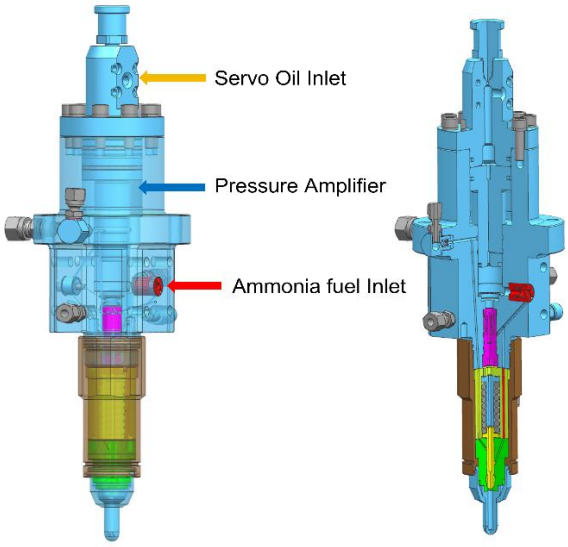

Figure 1. CPGC future fuel injector

The structural components designed for the injector's primary injection function, along with a detailed schematic of its working principle, are shown in Figure 2. Before the start of fuel injection, the small piston chamber of the pressure amplifier is filled with low-pressure future fuel. After the booster control valve is energized, the medium-pressure servo oil (about 300 bar) passes through the A port of control valve. Then, it connects with the injector through the high-pressure pipeline. The servo oil enters the large piston chamber of the pressure amplifier. It acts on the large piston to promote the movement of the large piston and realize the pressurization process of the future fuel. When the fuel pressure reaches the opening pressure of the fuel valve, the fuel enters the high-pressure fuel channel. As the pressure further increases to the opening pressure of the needle valve, the needle valve is lifted to achieve fuel injection. When the target injection quantity is completed, the boost control valve is powered off and closed, and the servo oil is returned to the low-pressure fuel tank through the control T port. Currently, the servo oil pressure in the booster chamber decreases rapidly, and the future fuel pressure decreases accordingly. The injection process ends after the needle valve is closed and the oil outlet valve is closed. The closing sequence of the needle valve and the fuel outlet valve ensures that the pressure in the high-pressure fuel flow channel is maintained at a certain level,

ensuring that the injector's future fuel is not prone to gasification.

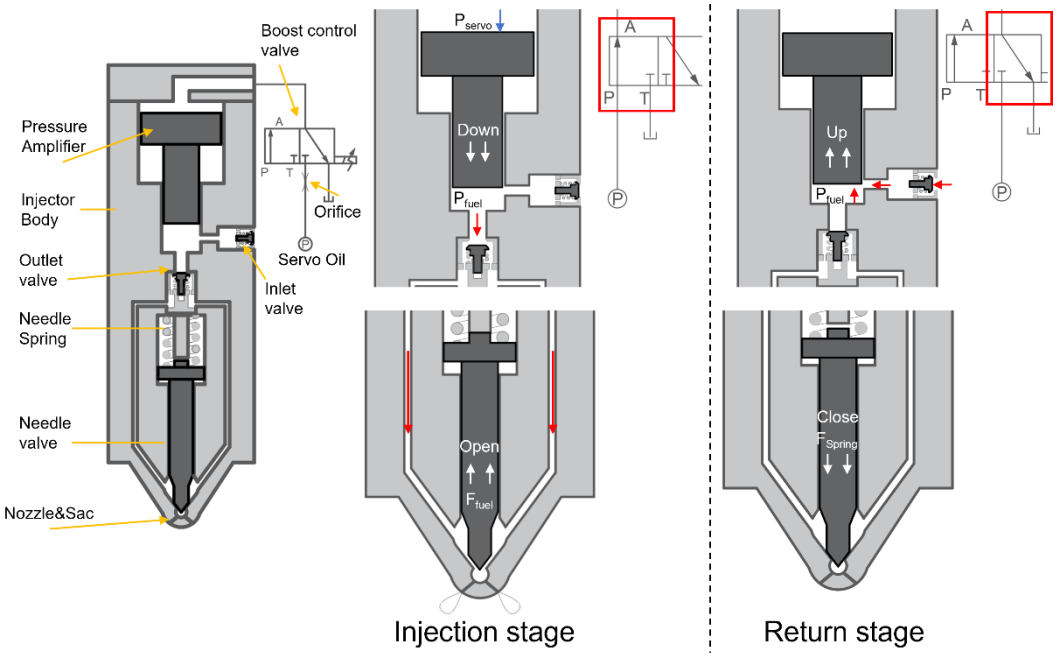

Figure 2. Schematic diagram of the working principle of the future fuel injector

3 MODELLING THEORY AND METHODOLOGY

A mathematical model of the injection system was constructed to study the influence of the thermal environment on the injection performance of future fuel injectors. The model uses a one-dimensional pipeline flow model and a lumped parameter modeling method for moving parts; considering the influence of fuel properties with temperature and pressure changes and wall convection heat transfer, the equations used in the modeling process are as follows:

Modeling of flow in fuel pipes considering cavitation:

The flow of high-pressure fluid in the servo oil high-pressure pipes and the internal flow channel of the injector can be described by a one-dimensional pipeline model, which is defined by three control equations when considering the effect of temperature, namely fluid continuity equation, momentum equation, and energy conservation equation. By discretizing the one-dimensional pipeline into computational grids, the partial differential equations of each control unit can be simplified into ordinary differential equations, thereby improving the computational efficiency. The specific form of the equation is as follows :

continuity equation:

$$\frac{dp}{dt} = \beta_{\text{eff}} \cdot \left(\frac{\Sigma dm_i}{\rho V_{\text{eff}}} + \alpha \frac{dT}{dt} + \rho \Sigma \frac{1}{\rho_v} . \frac{dx_v}{dt} \right) \quad (1)$$

Where p is the mean pressure at the flow cross-section, t denotes time, β_{eff} is the fluid/pipe effective bulk modulus, Σdm_i is the sum of incoming mass flow rates, ρ is the mean density at the flow section, V_{eff} is the effective volume of pipe, T is the internal temperature of the pipeline, α is the volumetric expansion coefficient, ρ_v and x_v denote the mass fraction and density of vapor, and x_v can be calculated by m_v / m_f , with m_v and m_f are vapor mass and fluid mass, respectively.

Momentum equation：

$$\frac{d(dm)}{dt} = A . \frac{p_1 - p_2}{l} - f . \frac{A}{D} \frac{v|v|}{2} . \rho \quad (2)$$

Where A is the cross-sectional area of the pipeline, p_1 and p_2 are are the pressures at both ends of the pipeline section, l refers to the length of the pipeline, f is the flow friction coefficient, D is the internal diameter of the pipe, and v represents the mean flow velocity across the flow cross-section.

Conservation of energy：

$$\frac{dT}{dt}=\frac{\dot{Q}+\Sigma dmh_i-h\sum dm_i}{\rho c_p V_{\text{eff}}}+\frac{\alpha T}{\rho c_p}\frac{dp}{dt}-\frac{1}{c_p}\sum h_v.\frac{dx_v}{dt} \quad (3)$$

Where $\dot{Q}$ signifies the heat exchanged with outside, Σdmh_i denotes the sum of incoming enthalpy flow rates, h is the mass enthalpy, c_p refers to the specific heat of the fluid, and h_v refers to the specific enthalpy of the vapor.

When the volume fraction of fluid cavitation is tiny, steam's influence on the fluid's physical properties in the cavitation state can be simplified as a uniform mixture of pure liquid and steam. In this case, by introducing the volume fractions of the gas and liquid phases as variables, the density of the cavitating fluid can be expressed by the following equation :

$$\rho_f=\frac{1}{\frac{x_l}{\rho_l}+\frac{x_v}{\rho_v}} \quad (4)$$

Where ρ_f is the fluid density, x_l represents the liquid mass fraction, and ρ_l is used to show the density of pure fluid. The density of the gas satisfies the ideal gas equation of state in the form shown below:

$$\rho_v(p,T)=\frac{p}{r_v T}, r_v=\frac{R}{M_v} \quad (5)$$

The convective heat transfer between the high-pressure fuel and the pipe wall during the flow in the pipe can be regarded as the forced convective heat transfer in the circular pipe, so the empirical formula of the forced convective heat transfer coefficient in the circular pipe can be used to describe it. For the convective heat transfer in the irregular cavity, such as the pressurized chamber and the delivery chamber, the CFD simulation and the formula shown in Eqs(6) are used to calculate. is used to calculate the average convective heat transfer coefficient.

$$\dot{Q}=h_{pipe}\cdot A\cdot(T_{wall}-T) \quad (6)$$

Where h_{pipe} signifies the heat transfer coefficient of pipe, T_{wall} is the wall temperature of the pipe, and h_{pipe} can be calculated by Eqs. (7).

$$h_{pipe}=\frac{Nu.\lambda}{D} \quad (7)$$

Where Nu represents the Nusselt number, λ refers to the thermal conductivity.

In the simulation process, the hydraulic pressure of all the moving valves can be considered as the force of the piston under the same effective area. Therefore, the motion law of the valve can be described by the motion equation of the second-order system. The specific form is as follows :

$$m_m\frac{d^2X_m}{dt^2}+R_m\frac{dX_m}{dt}+K_mX_m+F_0=\sum_k p_k A_{m_k} \quad (8)$$

The left side of the Eqs. (8) is composed of the inertial force term, damping force term, elastic force term, and external bias force term, respectively, and the sum of these four forces is equal to the force of fluid. Where m_m represents the equivalent mass of the moving valve parts, R_m is the resistance coefficient of the valves in motion, K_m means the equivalent stiffness coefficient of the system, indicating that the motion valve is affected by the elastic restoring force, X_m refers to the displacement of moving valve parts, p_k is the fluid pressure of different chambers, A_{m_k} denotes the effective area between fluid and moving valve parts.

Fuel Properties:

The physical properties of ammonia fuel are highly sensitive to temperature, and the traditional polynomial equation cannot accurately describe the nonlinear trend of its physical parameters with pressure and temperature. The Tait equation can be used to describe the compressibility of most fluids under different pressure and temperature conditions, especially in characterizing fluid characteristics under high-pressure conditions. The typical form of Tait equation is shown in Eqs. (9).

$$\rho=\frac{\rho_0}{1-C\cdot\ln\frac{B+P}{B+P_0}} \quad (9)$$

Where, ρ_0 is the reference density and P_0 is the reference pressure, usually ρ_0 and P_0 are taken as the saturation pressure and its corresponding density at a certain reference temperature, which is a fixed value. In contrast, for ammonia fuel, its saturation pressure varies significantly with the temperature and is strongly nonlinear. The traditional reference density and reference pressure defined through constants cannot accurately describe its physical characteristics, so

the Antoine equation describes saturation pressure as a function of temperature shown in Eqs. (10), then the relationship between density and temperature in the saturated state is fitted through the equation shown in Eqs. (11), which is improved by bringing it into the Tait equation.

$$P_0 = P_{sat} = f_1(T) = 10^{(a_1 - \frac{b_1}{T + c_1})} \quad (10)$$

$$\rho_0 = \rho_{sat} = f_2(T) = a_2.(1 - b_2 T)^{c_2} \quad (11)$$

Where P_{sat} denotes the saturation pressure of ammonia fuel, T refers to the temperature of ammonia fuel, a , b and c are the empirical fitting parameters of Antoine equation, which are determined by the experimental data.

Based on the above fitting method, the fitting results of the physical properties of ammonia fuel are obtained. The fitting results of density and specific heat are shown in the following Figure:

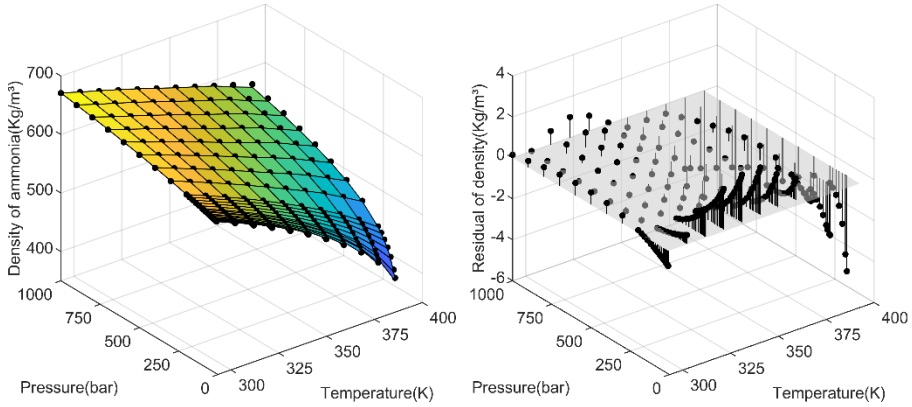

Figure 3. Ammonia fuel density fitting results

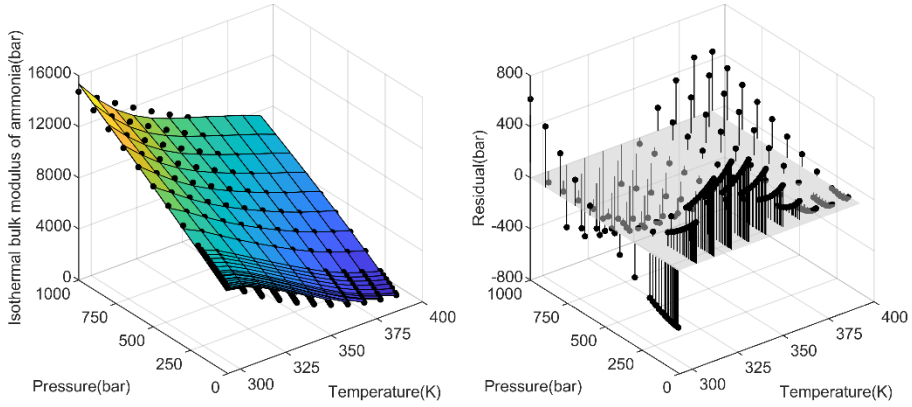

Figure 4. Ammonia fuel bulk modulus fitting results

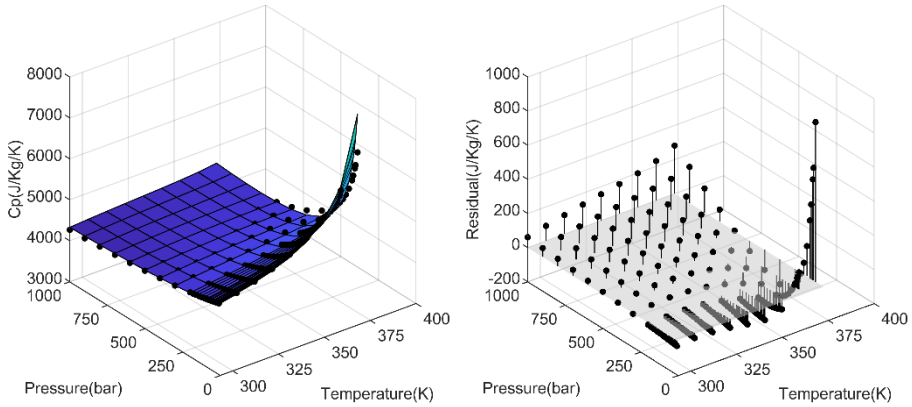

Figure 5. Ammonia fuel specific heat fitting results

As can be seen from the Figure, the physical properties of the ammonia fuel fitted using this physical property equation have a high accuracy under the operating conditions of the engine, for the density fitting results, the R^2 reached 0.99998, and the AAD was 0.15 %. For the isothermal bulk modulus fitting results, the R^2 is 0.9933, and the AAD is 5.7 %. For the specific heat fitting results, the R^2 is 0.9968, and the AAD is 1.37 %.

To consider the influence of a high-temperature environment on the process of ammonia fuel injection during the cycle injection duration, a CFD model of the fluid domain in the pressurization chamber during the process of methanol pressurization and absorption was established, and the dynamic mesh boundary simulated the motion of the pressurized piston. Then, the convective heat transfer inside the pressurized chamber during the pressurization and oil absorption process is simulated, and then the convective heat transfer coefficient of the pressurized chamber suitable for one-dimensional simulation is obtained. At the same time, the flow and heat transfer in the delivery chamber and the Sac chamber are also considered; the actual flow around the needle valve and nozzle positions, after the needle valve opens, was simulated, enabling the correction of the convective heat transfer coefficient in the one-dimensional simulation. The fluid domain and wall setting in CFD calculation are shown in Figure 6.

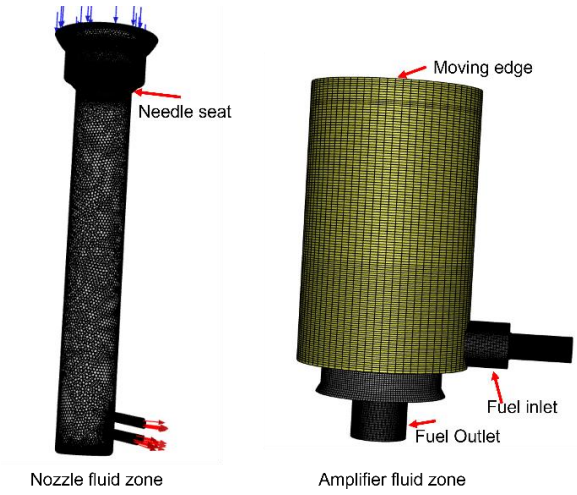

Figure 6. Fluid domain of CFD convective heat transfer calculation

To analyze the influence of wall temperature on the characteristics of the ammonia fuel injection process, considering the temperature difference in different regions of the injector, the temperature boundary conditions are divided according to the relative position of the injector installation and the corresponding steady-state wall temperature is set for different regions, so that the simulation results are closer to the actual situation. The wall temperature setting is shown in Figure 7, and the temperature data refer to the existing research literature on the nozzle temperature of the injector [8].

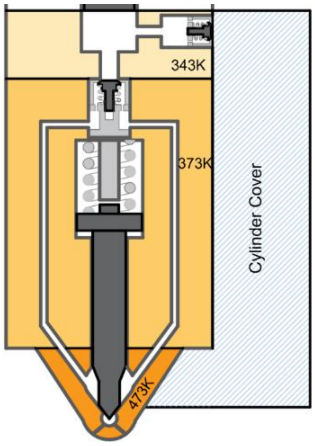

Figure 7. Wall temperature boundary conditions for ammonia fuel injection performance calculation

4 SIMULATION RESULTS ANALYSIS

4.1 Convective heat transfer of ammonia fuel boost and injection process

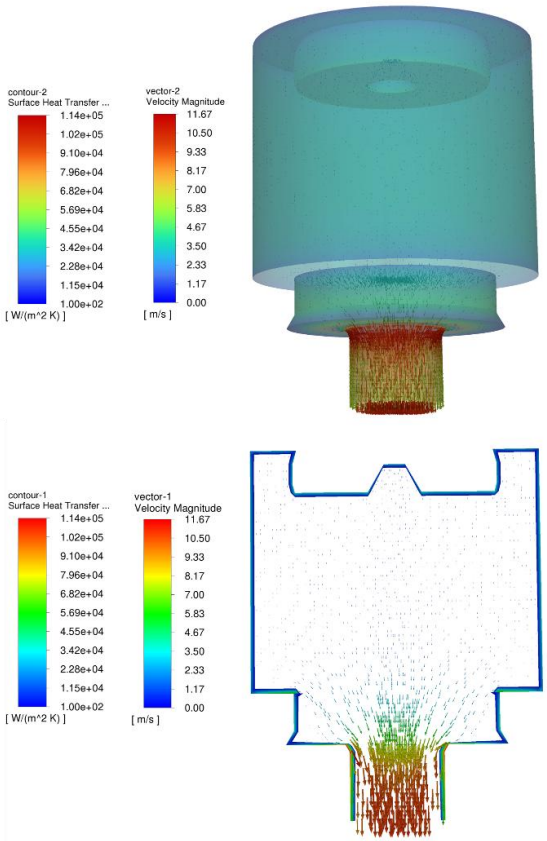

Figure 8. Convective heat transfer coefficient and velocity distribution in the pressurization process of plunger chamber

The injector achieves the intake and discharge of ammonia fuel through the reciprocating motion of a pressurizing plunger, combined with the opening and closing of check valves for the inlet and outlet. During the stable phases of the pressurization and fuel suction processes, the velocity of the plunger is kept constant, and the velocity of the plunger is determined by the injection volume flow rate of the ammonia fuel and the pressure of the ammonia fuel during fuel absorption. In different stages of plunger motion, there are significant differences in the direction and velocity of fuel flow in the plunger chamber. For these characteristics, the fluid domain is established for the pressurization and fuel absorption processes, respectively, for simulation. Considering that the convective heat transfer mainly occurs at the solid wall surface, a boundary layer grid is set at the plunger chamber's wall surface and the fuel's inlet and outlet to accurately calculate the convective heat transfer phenomenon at the wall surface.

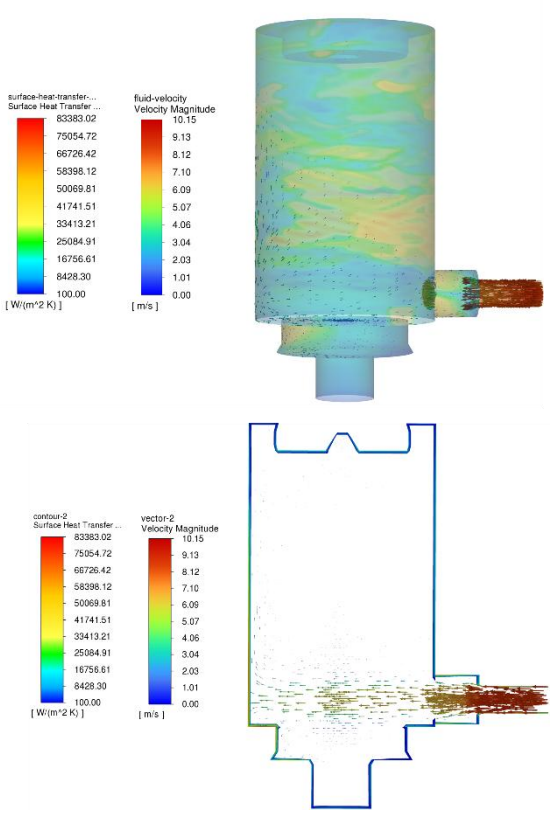

Figure 9. Convective heat transfer coefficient and velocity distribution of fuel absorption process in the plunger chamber

The CFD simulation results are shown in Figure 8 and Figure 9. It can be seen from the CFD calculation results that during the pressurization process, due to the throttling effect of the fuel outlet valve, the fluid velocity in the plunger chamber is low. The velocity gradient near the wall is slight, the maximum fluid velocity appears at the outlet of the plunger chamber, where the velocity gradient near the wall increases significantly, the boundary layer is thinner. The shear rate of the fluid is higher. Therefore, this position's convective heat transfer coefficient is significantly higher than that in the plunger cavity wall. In the process of plunger fuel absorption, low-pressure ammonia fuel flows into the chamber through the lateral fuel inlet valve and forms a jet along the radial direction of the plunger in the chamber. This jet causes a significant disturbance of the fluid in the plunger chamber. It increases the velocity gradient near each wall, significantly increasing the convective heat transfer coefficient at multiple locations in the plunger chamber. Furthermore, since the velocity of the plunger in the pressurization process (1 m/s) is greater than that in the oil absorption process (0.25 m/s), the overall convective heat transfer coefficient in the plunger chamber during the pressurization process is significantly higher.

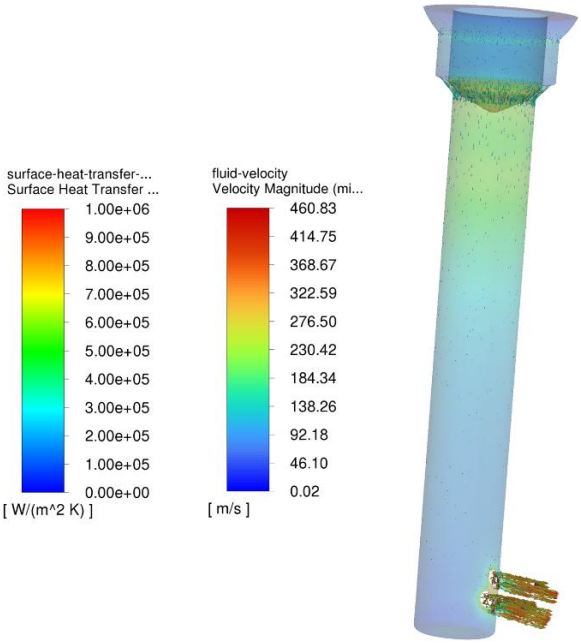

Figure 10. Distribution of convective heat transfer coefficient and flow velocity within the needle valve and sac chamber during the injection process

Figure 10 illustrates the distribution of the convective heat transfer coefficient within the needle valve and the Sac chamber during the injection process after the needle valve opens. The calculation results show that the convective heat transfer coefficient in the flow channel of the needle valve and the Sac chamber is much higher than that in the plunger chamber. This is mainly due to the design characteristics of the injector; the flow area of the flow channel decreases step by step from top to bottom, resulting in the fluid velocity at the needle valve and nozzle being much larger than other positions inside the injector. At the needle

valve, the fluid flow presents a strong turbulent state with a high Reynolds number, so the convective heat transfer at the needle valve is the most significant. In Figure 10, except for the nozzle hole, the convective heat transfer coefficient at the minimum throttling position of the needle valve seat is the largest. As the fluid flow rate gradually decreases behind the valve seat, the convective heat transfer coefficient decreases gradually.

To incorporate the CFD results of convective heat transfer into one-dimensional calculations, the volume-averaged convective heat transfer coefficient is introduced to process the CFD data. The definition of the volume-averaged convective heat transfer coefficient is as follows:

$$h_{avg} = \frac{q_{total}}{A_w (T_w - T_{in})} \tag{12}$$

Where q_{total} denotes the total heat flux in the chamber, A_w represents the total heat transfer area of the chamber, T_w and T_{in} correspond to the wall temperature of the chamber and the fluid temperature at the inlet of the chamber, respectively.

According to the definition of convective heat transfer coefficient, the average values of three different local convective heat transfer coefficients are calculated, as shown in Table 1:

Table 1. The average value of local convective heat transfer coefficient

Location of CHTC	Unit	Value
Boost process of amplifier chamber	W/(K.m^2)	30163.1
Return process of amplifier chamber	W/(K.m^2)	18829.1
Needle valve & Sac	W/(K.m^2)	290942.6

4.2 Pressure building and injection characteristics of ammonia fuel

Figure 11. shows the injection performance of the future fuel injector with ammonia as fuel calculated based on the one-dimensional flow characteristic prediction model considering heat transfer mentioned above, including the pressure time history of different positions inside the injector during the injection process and the motion law of key components. As can be seen in Figure 11, after the pressurized control valve pilot valve is actuated, the servo oil pressure in the pressurized chamber starts to increase after about 3.7ms. Then, the pressurized plunger starts to act, and the ammonia fuel pressure gradually increases. Figure 12 shows the motion law of the pressurized plunger during the injection process; from the diagram, it can be seen that the pressurization process accelerates at the initial stage of pressurization. After reaching a peak speed, the pressure of ammonia increases this time. Still, the injection rate of ammonia fuel is less than the volume change rate of the pressurized piston at this peak speed, so the pressurized piston begins to slow down. At this time, the flow rate of servo oil in the servo oil supply pipeline decreases, which leads to the phenomenon of water hammer in the servo oil pipeline, which causes the pressure fluctuation of servo oil pressure and further causes the pressure fluctuation of ammonia fuel, as shown in the calculation results in Figure 11. In the process of system matching, the throttle hole is set at the P port of the control valve, which can effectively suppress the flow rate and velocity of the servo oil flowing into the pressurization chamber at the initial stage of pressure building, thus inhibiting the further amplification of pressure fluctuation. When the plunger speed reaches stability, the injection pressure tends to be stable.

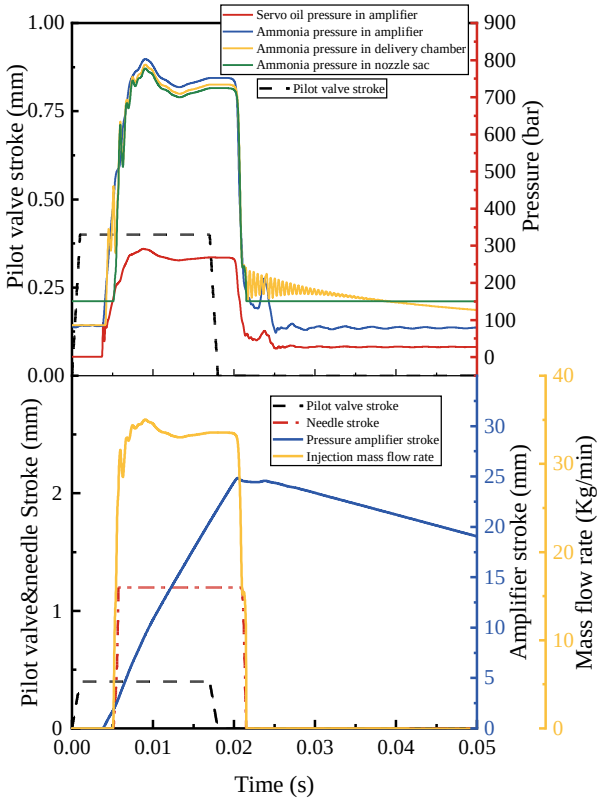

Figure 11. Dynamic injection characteristics of ammonia fuel (P_{servo} = 280, ET = 17ms)

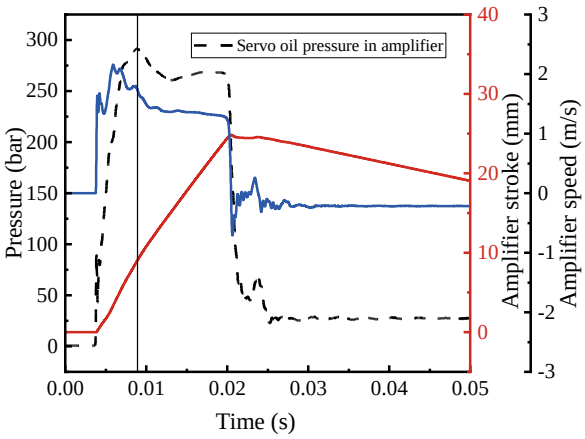

Figure 12. Pressurized plunger motion during ammonia fuel injection (P_{servo} = 280, ET = 17ms)

When the pilot valve of the pressurization control valve is closed, the servo oil pressure decreases after a delay of 3ms, and the ammonia fuel pressure also decreases. Then, the injector needle valve is closed, and the injection ends. The fuel outlet valve is closed after the needle valve to ensure that the pressure in the high-pressure ammonia fuel channel and the delivery chamber in the injector does not decrease with the decrease of the ammonia fuel pressure in the pressurization chamber, and remains at a certain pressure level before the next cycle of injection.

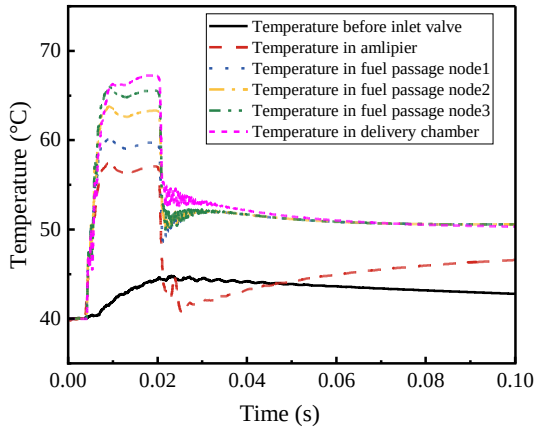

Figure 13. The distribution of ammonia fuel temperature along the ejector injection process

Figure 13 shows the temperature distribution of ammonia fuel at different positions along the ammonia fuel injection loop in the injector. The supply condition of ammonia is 85 bar,40 °C. It can be seen from the diagram that during the pressurization process, due to the work of the pressurized plunger on the ammonia fuel, the pressure and temperature of the ammonia fuel increase significantly, and the peak temperature of the ammonia fuel in the pressurized chamber reaches 57.5 °C. At the same time, due to the convective heat transfer with the wall of the injector, the temperature of the ammonia fuel gradually increases along the different positions of the high-pressure oil channel. The maximum temperature in the delivery chamber can reach 67.3 °C, which is 27.3 °C higher than the supply temperature. In addition, during the pressurization process, the high-pressure ammonia fuel leaks to the front area of the fuel suction valve through the plunger gap, increasing the temperature of the region. After the servo oil is depressurized, the high-pressure ammonia fuel expands rapidly, and its pressure and temperature decrease quickly.

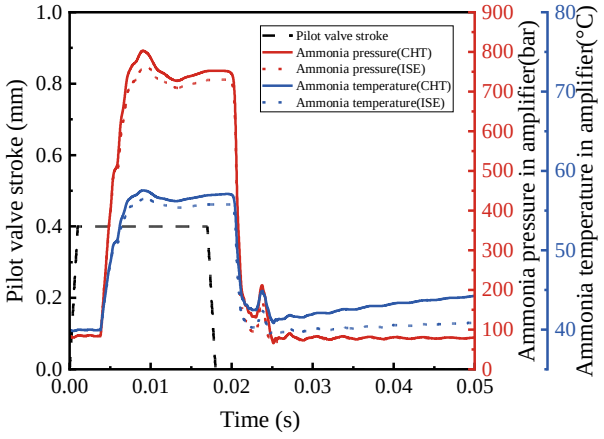

a. Pressure amplifier chamber

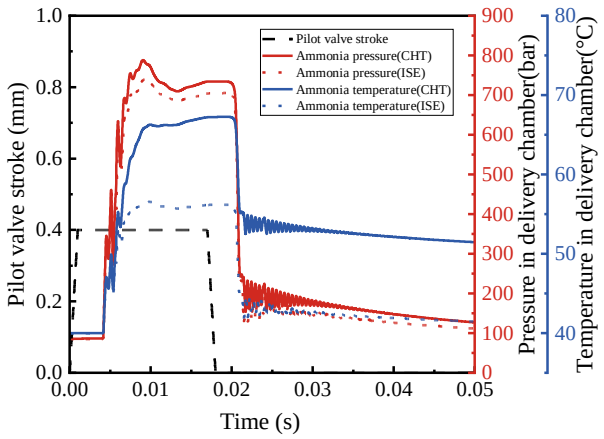

b. Fuel delivery chamber

Figure 14. Comparison of calculation results between convective heat transfer (CHT) flow model and adiabatic (ISE) model

To emphasize the influence of convective heat transfer on the temperature rise in the ammonia fuel injection process, an adiabatic flow simulation model of ammonia fuel injection was established. The convective heat transfer process with or without a wall surface and its influence on the

characteristics of ammonia fuel injection were compared under the same operation conditions.

Figure 14 compares the convective heat transfer (CHT) flow model and the adiabatic flow (ISE) model to predict the ammonia fuel injection characteristics. It can be seen that when considering the heat transfer in the pressurized chamber and the high-pressure flow channel, the pressure peak of the ammonia fuel in the pressurized chamber increases, and the temperature peak increases by 1.3 °C compared with the adiabatic condition. The reason is that the wall heat transfer increases the temperature of the ammonia fuel in the pressurized chamber, which leads to the increase of the pressure due to the thermal expansion. From the comparison of the temperature distribution of ammonia fuel in the delivery chamber, it can be seen that the convective heat transfer is more intense in the high-pressure fuel channel and the delivery chamber, resulting in an increase of 11 °C in the temperature of the delivery chamber compared with the adiabatic condition. Similarly, the fuel pressure in the delivery chamber also increased due to thermal expansion.

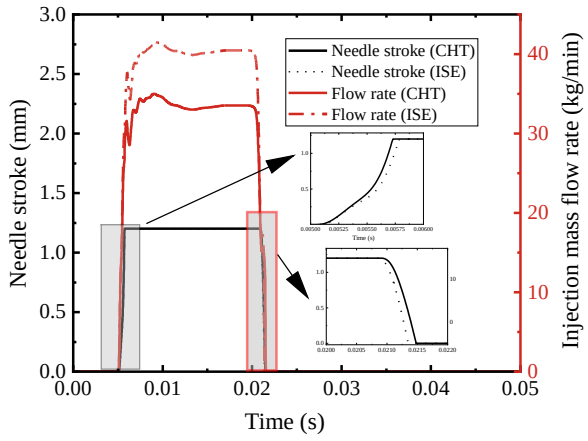

Figure 15. Comparison of injection rate and needle valve motion between convective heat transfer flow model and adiabatic model

The temperature rise caused by convective heat transfer will significantly affect the injection characteristics of ammonia fuel, as shown in Figure 15. Among them, the most significant change caused by the increase in fuel temperature is the difference in the mass flow rate of ammonia fuel injection. The diagram shows that when the wall heat transfer is considered, the injection mass flow rate of ammonia fuel is reduced by 7 kg/min, which is 17.4 % lower than that under adiabatic conditions. In addition, the thermal expansion caused by the increase in fuel temperature slightly affects the needle valve's response. Compared with the adiabatic condition, the opening response of the needle valve is advanced, and the closing response is delayed after considering the heat transfer. The change in ammonia fuel pressure causes this phenomenon.

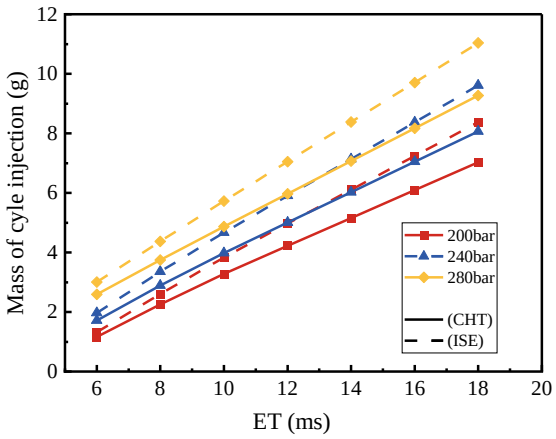

Figure 16. Convective heat transfer flow model and adiabatic model injection quantity calculation results

To highlight the influence of convective heat transfer on the injection characteristics of ammonia fuel, the cyclic injection quantity of ammonia fuel was calculated using these two models under different injection pressures and injection pulse widths. It can be seen from Figure 16 that the influence of wall heat transfer on the injection quality of the ammonia fuel cycle is similar under different injection pressures. Since the wall heat transfer directly affects the size of the injection mass flow rate, as the injection pulse width increases, the difference in fuel injection volume predicted by the two models also increases. The maximum difference of the cycle injection quantity is 1.76 g, accounting for 16 % of the cycle injection quantity.

The above analysis results show that the wall heat transfer phenomenon significantly affects the injection characteristics of ammonia fuel, especially under the condition of a large pulse width. The temperature effect needs to be considered and corrected accordingly in the engine control strategy.

4.3 Effect of Ammonia Fuel Supply Temperature

To ensure the phase stability of the ammonia fuel supply, the supply pressure of ammonia fuel on the main engine is usually between 50 bar and 90 bar, and the supply temperature is between 25 °C and 60 °C. Based on the current simulation model considering the wall heat transfer effect, the influence of different supply temperatures on the

injection characteristics of ammonia fuel is analyzed. The results are as follows:

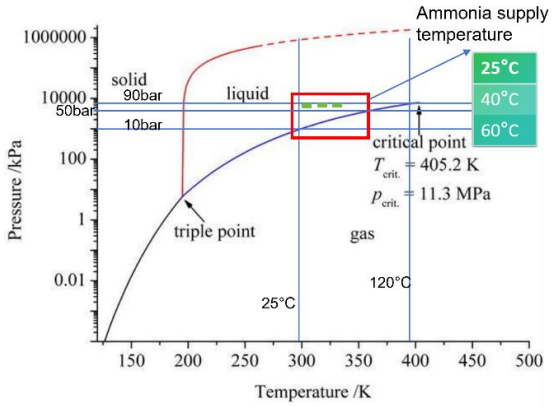

Figure 17. The supply temperature of different ammonia fuels

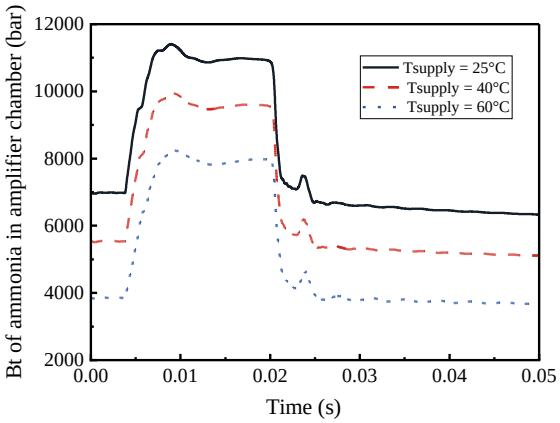

Figure 19. Variation of the elastic modulus of ammonia fuel with supply temperature

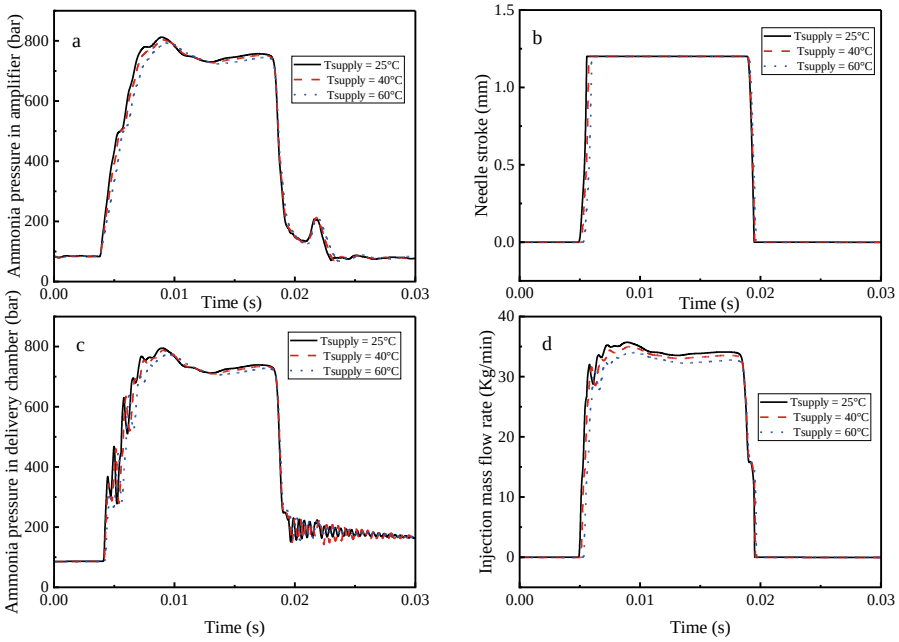

Figure 18. The effect of ammonia fuel supply temperature on injection characteristics (P_{supply} = 85 bar).

It can be seen from Figure 18 that the pressure-building characteristics of ammonia fuel vary under different supply temperatures. After the supply temperature increases, the pressurization curve of the ammonia fuel becomes more gentle, and the injection response delay of the ejector increases. The reason should be that the increase in supply temperature significantly affects the bulk elastic modulus of ammonia fuel, which leads to the change of compressibility and sound velocity of ammonia fuel, as shown in Figure 19. In addition, the increase in the supply temperature reduces the fuel density, resulting in a decrease in the injection mass flow rate. Therefore, the change in ammonia fuel supply temperature will affect the injection timing and injection quantity of the injection system.

4.4 Comparison of injection and pressure fluctuation characteristics of diesel and ammonia fuels

There are apparent differences in diesel and ammonia fuels' physical and chemical properties. Under the same temperature and pressure, diesel parameters, such as density and bulk modulus, are

much larger than those of ammonia fuel. The purpose of this section is to analyze the difference in injection characteristics between diesel and ammonia under the same working conditions without changing the structural parameters of the system, which provides a reference for the design of flexible fuel injection characteristics of the injector.

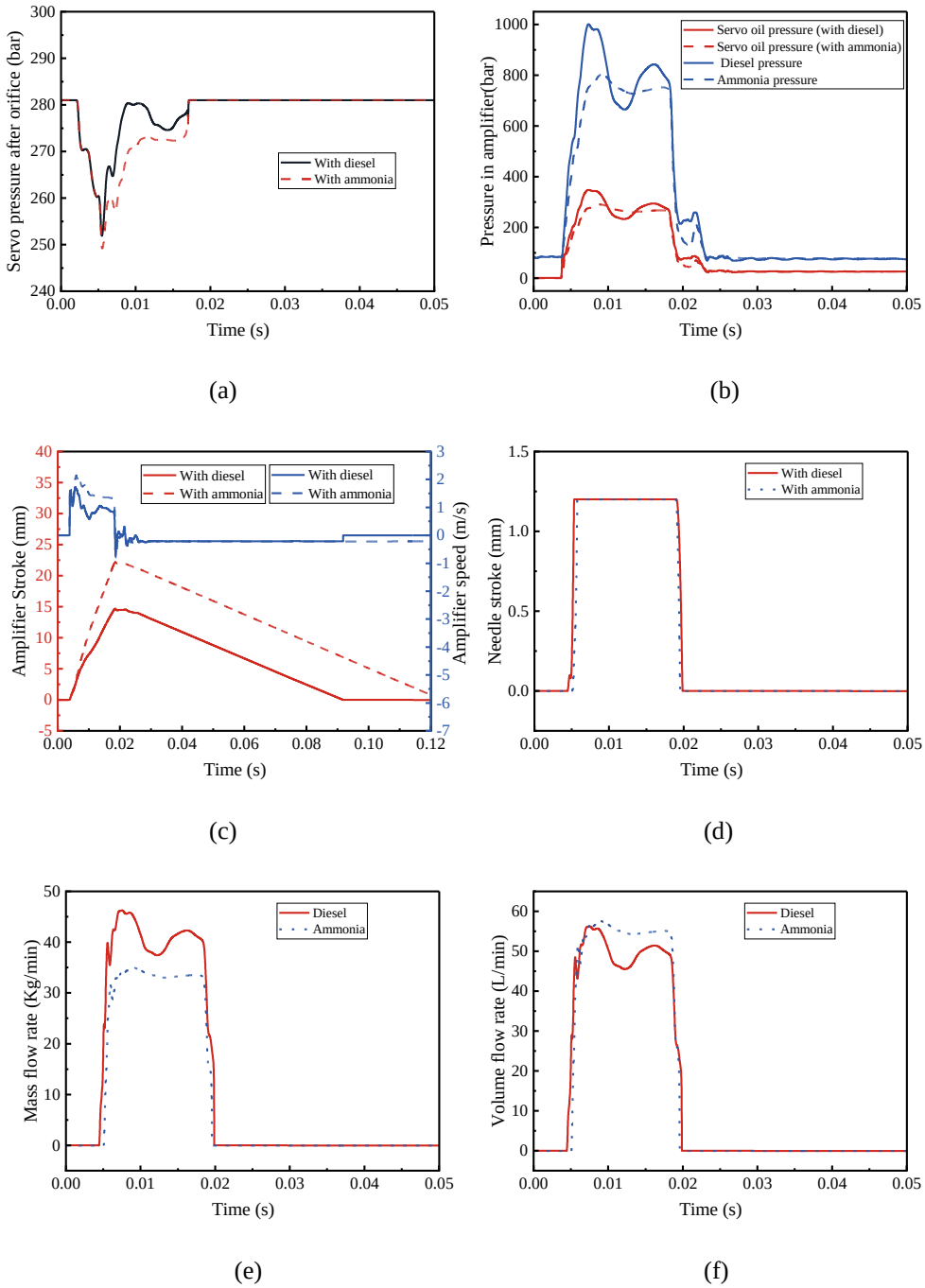

Figure 20. Comparison of injection characteristics of diesel and ammonia

Figure 20 compares the pressurized injection characteristics of diesel and ammonia fuel under servo oil pressure of 280 bar and injection pulse width of 17 ms. It can be seen from the Figure that when the same injection system structure is used, there are significant differences in the dynamic injection characteristics of diesel and ammonia fuels. Under the same servo oil pressurization supply condition, the pressure fluctuation amplitude after diesel pressurization is larger. In addition, the pressure fluctuation trends of the two fuels in the servo oil pressurization chamber are different. When using diesel fuel, the stroke of the pressurized piston is smaller and the speed is lower, but the fluctuation of the speed is more intense, and the response speed of the needle

valve is faster in the diesel fuel mode. In terms of injection rate, the mass flow rate of diesel injection is more significant, while the volume flow rate is smaller.

The differences in the properties of diesel and ammonia fuels should explain the above differences. The density of diesel fuel is higher, at the target injection pressure of 700 bar, the density of diesel fuel is about 850 kg / m3, while the density of ammonia fuel is about 610 kg / m3; the density difference between the two determines that the diesel fuel has a larger fuel injection mass flow rate and a smaller volume flow rate at the same injection pressure. In the pressurized fuel injection system, the volume flow rate and the circulating injection volume determine the running speed and maximum stroke of the pressurized plunger. Therefore, in the diesel mode, the stroke and speed of the pressurized plunger are small. For the pressurized injection system, the pressure fluctuation cannot be explained only by the water hammer phenomenon of the high-pressure supply pipeline. More important is the interaction between the two oils (servo oil and fuel oil) and the relationship with the motion characteristics of the pressurized plunger. In the initial pressure build-up period of the pressurized injection system, the pressure in the servo oil pressurized chamber increased from the return oil pressure of 1 bar to the supply pressure. In this process, the pressure of the fuel oil is lower than that of the servo oil, which causes the pressurized plunger to accelerate upward. At this time, due to the significant pressure difference between the front and rear of the control valve, the supply flow rate of the servo oil side is large. When the speed of the pressurized plunger increases to a certain value, the pressure of the pressurized fuel continues to increase because the volume change rate of the pressurized chamber is much larger than the fuel injection rate, resulting in a deceleration of the piston until the volume change rate of the pressurized chamber matches the injection rate. During the deceleration process, the servo oil supply flow rate decreases, resulting in a positive water hammer effect in the servo oil supply pipeline, resulting in a pressure fluctuation peak in the servo oil pressurized chamber pressure and the fuel chamber pressure. As seen in the dynamic injection characteristics in Figure 20 and Figure 12, the pressurization pressure peak corresponds to the pressurization plunger's deceleration phase.

In the system design, the servo oil supply capacity is adjusted according to the properties of ammonia fuel to meet the needs of ammonia fuel injection. Due to the density difference between the two fuels, it can be seen that under the same injection pressure, the volume flow rate of diesel is smaller, and the servo oil supply required for stable injection is also smaller. Therefore, when diesel fuel is used, in the initial stage after the control valve is opened, the servo oil flow rate is similar to that when ammonia fuel is used due to the pressure in the servo oil pressure chamber both are return oil pressure. In the deceleration phase, the required supply needs to be reduced to a lower level, leading to more severe water hammer pressure fluctuations in the servo oil supply loop. In addition, the bulk modulus of diesel is larger, so the hydraulic pressure fluctuation generated in the deceleration stage of the supercharged piston is greater. Under the combined action of these two factors, the amplitude of pressure fluctuation during diesel injection increases significantly.

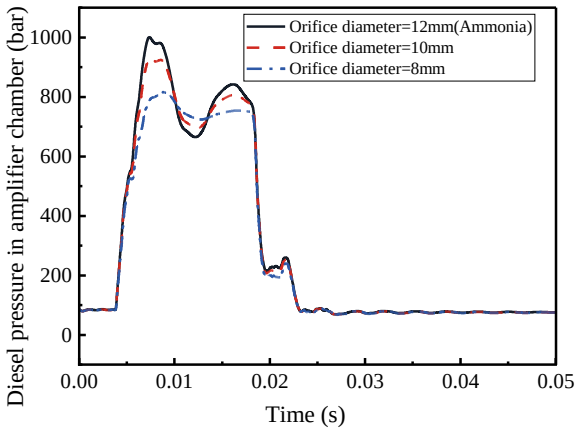

Figure 21. Diesel Boost Pressure at Different P-port Orifice Diameters

Based on the above analysis, the servo oil supply capacity should be reduced when using diesel fuel. In practical design, this can be achieved by adjusting the diameter of the throttle orifice at the inlet of the pressurization control valve. By restricting the servo oil flow into the injector during the initial pressurization phase, pressure stabilization can be effectively achieved; the inhibition effect is shown in Figure 21.

5 CONCLUSIONS

In this study, based on the structure of the pressurized ammonia fuel injector, a prediction model of ammonia fuel characteristics and a CFD model of convective heat transfer in key heat exchange chambers were developed. Combining it with the one-dimensional pipeline flow theory, a one-dimensional simulation model of ammonia fuel injection characteristics considering the influence of convective heat transfer is established. Through this model, the influence of wall convective heat transfer on the injection characteristics of ammonia fuel and the influence of ammonia fuel supply temperature on the injection performance are studied. Finally, the difference between the

injection characteristics and pressure fluctuation characteristics of the pressurized ammonia fuel injection system when using diesel and ammonia fuel is analyzed. The main conclusions of this paper are as follows :

1. The ammonia fuel property model, developed by improving the Tait equation, demonstrates high accuracy and can effectively predict the physical properties of ammonia fuel within the fuel injection system's pressure and temperature operating range. Simulation results of convective heat transfer at the pressurization chamber and needle valve positions indicate that the convective heat transfer intensity during pressurization is higher than during the fuel suction process. Due to the smaller flow area at the needle valve position, the fluid velocity is higher, resulting in a convective heat transfer coefficient at this location being an order of magnitude greater than that within the pressurization chamber.

2. Based on a one-dimensional simulation model, the dynamic injection characteristics of ammonia fuel were analyzed. The results show that the pressure fluctuations of ammonia fuel during the injection process are primarily caused by changes in fluid velocity within the servo oil high-pressure pipeline, induced by the acceleration and deceleration of the pressurization piston, leading to water hammer pressure fluctuations. During the pressurization and injection of ammonia fuel, the fuel temperature in the delivery chamber increases by 27.3°C compared to the supply temperature and by 11°C compared to the adiabatic flow process due to the work done by the plunger and convective heat transfer. The impact of convective heat transfer on the injection characteristics of ammonia fuel is significant. At rated load, considering convective heat transfer, the ammonia fuel injection mass flow rate decreased by 17.4%, with the maximum difference in cyclic injection volume reaching 1.76g, a reduction of 16%. The pressure variation caused by convective heat transfer also influences the needle valve opening and closing response times.

3. The analysis of injection characteristics under different ammonia fuel supply temperatures reveals that an increase in supply temperature significantly affects the bulk modulus, resulting in a greater injection response delay. Additionally, changes in supply temperature directly influence the mass flow rate of ammonia fuel, which further impacts the injection timing and the quantity of fuel injected within the system.

4. When using an injection system with identical structural parameters, the injection characteristics of diesel and ammonia fuel exhibit significant differences under the same operating conditions. These differences primarily stem from variations in density and bulk modulus between diesel and ammonia fuel, which lead to notable discrepancies in servo oil supply quantities and pressure fluctuation, which causes the injection characteristics of the two fuels to differ substantially. When switching to the diesel fuel model, it is necessary to reduce the servo oil supply in the ammonia fuel injection system. This can be achieved by installing a throttling orifice at the control valve to mitigate pressure fluctuation issues in diesel mode.

The next phase will involve experimental testing of the boosted ammonia fuel injection system. Through these tests, further studies on the pressure fluctuation patterns in the ammonia fuel injection system will be conducted, and the influence of fuel properties, ambient temperature, and other factors on the fuel system's injection characteristics will be analyzed, thereby providing guidance for the conceptual design and structural optimization of flexible fuel injectors.

6 DEFINITIONS, ACRONYMS, ABBREVIATIONS

RSME: Root Mean Square Error

AAD: Average Absolute Deviation

R^2: Coefficient of Determination

ET: Energizing Time

CHT: Convective Heat Transfer

ISE: Isentropic

CHTC: Convective Heat-Transfer Coefficient

7 ACKNOWLEDGMENTS

This work was supported by the National Natural Science Foundation of China (52401373), Heilongjiang Provincial Postdoctoral Science Foundation (LBH-Z23119) and Postdoctoral Fellowship Program of CPSF (GZC20233430).

8 REFERENCES AND BIBLIOGRAPHY

[1] Joung, T.H., Kang, S.G., Lee, J.K., et al. 2020. The IMO initial strategy for reducing Greenhouse Gas(GHG) emissions, and its follow-up actions towards 2050. Journal of International Maritime Safety, Environmental Affairs, and Shipping;4:1–7. https://doi.org/10.1080/25725084.2019.1707938.

[2] Zhou, X.Y., Li, T., Chen, R., et al. 2024. Ammonia marine engine design for enhanced

efficiency and reduced greenhouse gas emissions. Nat Commun 15:2110. https://doi.org/10.1038/s41467-024-46452-z.

[3] Valera-Medina, A., Xiao, H., Owen-Jones, M., et al. 2018. Ammonia for power. Progress in Energy and Combustion Science, 69:63–102. https://doi.org/10.1016/j.pecs.2018.07.001.

[4] Machaj, K., Kupecki, J., Malecha, Z., et al. 2022. Ammonia as a potential marine fuel: A review. Energy Strategy Reviews, 44:100926. https://doi.org/10.1016/j.esr.2022.100926.

[5] Sun, L., Xiong, Z., Qiu, J., et al. 2020. Corrosion behavior of carbon steel in dilute ammonia solution. Electrochimica Acta , 364:137295. https://www.sciencedirect.com/science/article/pii/S0013468620316881.

[6] Kurien, C., Mittal, M. 2022. Review on the production and utilization of green ammonia as an alternate fuel in dual-fuel compression ignition engines. Energy Conversion and Management , 251:114990. https://doi.org/10.1016/j.enconman.2021.114990.

[7] Sehili Y., Cerdoun, M., Loubar K., et al. 2024. Dual fuel engine injector temperature monitoring: An innovative thermal analysis approach. Applied Thermal Engineering , 249:123370. https://doi.org/10.1016/j.applthermaleng.2024.123370.

[8] Czarneski, F. E., Och, S. H., Moura, Luís M. 2015. Characterization of Nozzle Tip Temperature of Diesel Injector in a Dual Fuel Engine. 7th European Combustion Meeting, p. 1–6.

[9] Risberg, P. A., Adlercreutz, L., Aguilera, M. G., et al. 2013. Tobias Johansson, Lars Stensiö, Hans-Erik Angstrom. Development of a Heavy Duty Nozzle Coking Test, p. 2013-01–2674. https://doi.org/10.4271/2013-01-2674.

[10] Gao, K.H., Wu, J.T., Bell, I.H., et al. 2023. A Reference Equation of State with an Associating Term for the Thermodynamic Properties of Ammonia. Journal of Physical and Chemical Reference Data , 52:013102. https://doi.org/10.1063/5.0128269.

[11] Payri, R., García-Oliver, J.M., Bracho, G., et al. 2024. Experimental characterization of direct injection liquid ammonia sprays under non-reacting diesel-like conditions. Fuel, 362:130851. https://doi.org/10.1016/j.fuel.2023.130851.

[12] Payri, R., Salvador, F.J., Carreres, M., et al. 2018. An Investigation on the Fuel Temperature Variations Along a Solenoid Operated Common-Rail Ballistic Injector by Means of an Adiabatic 1D Model . SAE Technical Paper Series

[13] Cavicchi, A., Postrioti, L., Pesce, F.C., et al. 2018. Experimental Analysis of Fuel and Injector Body Temperature Effect on the Hydraulic Behavior of Latest Generation Common Rail Injection Systems. SAE Technical Paper Series

[14] Bae, G.H., Choi, S., Lee, S., et al. 2021. Experimental investigation of fuel temperature effects on transient needle motion and injection velocity of solenoid type diesel injector. International Journal of Heat and Mass Transfer , 181:121838. https://doi.org/10.1016/j.ijheatmasstransfer.2021.121838.

[15] Salvador, F. J., Gimeno, J., Martín, J., et al. 2020. Thermal effects on the diesel injector performance through adiabatic 1D modelling. Part I: Model description and assessment of the adiabatic flow hypothesis. Fuel ,260. https://doi.org/10.1016/j.fuel.2019.116348.

[16] Lan, Q., Fan, L.Y., Bai, Y., et al. 2021. Experimental and numerical investigation on pressure characteristics of the dual-valve controlled fuel system for low-speed diesel engines. Fuel ,294:120501. https://doi.org/10.1016/j.fuel.2021.120501.

[17] Bai, Y., Lan, Q., Fan, L.Y., et al. 2023. Pressure characteristics of the fuel system for two-stroke diesel engines under different operational modes. Fuel ,332:126007. https://doi.org/10.1016/j.fuel.2022.126007.